# Investigating Holey Metamaterial Effects in Terahertz Traveling-Wave Tube Amplifier

*David P. Starinshak*
*Ohio Aerospace Institute, Brook Park, Ohio*

*Jeffrey D. Wilson*
*Glenn Research Center, Cleveland, Ohio*

*Christine T. Chevalier*
*Analex Corporation, Cleveland, Ohio*

# NASA STI Program . . . in Profile

Since its founding, NASA has been dedicated to the advancement of aeronautics and space science. The NASA Scientific and Technical Information (STI) program plays a key part in helping NASA maintain this important role.

The NASA STI Program operates under the auspices of the Agency Chief Information Officer. It collects, organizes, provides for archiving, and disseminates NASA's STI. The NASA STI program provides access to the NASA Aeronautics and Space Database and its public interface, the NASA Technical Reports Server, thus providing one of the largest collections of aeronautical and space science STI in the world. Results are published in both non-NASA channels and by NASA in the NASA STI Report Series, which includes the following report types:

- TECHNICAL PUBLICATION. Reports of completed research or a major significant phase of research that present the results of NASA programs and include extensive data or theoretical analysis. Includes compilations of significant scientific and technical data and information deemed to be of continuing reference value. NASA counterpart of peer-reviewed formal professional papers but has less stringent limitations on manuscript length and extent of graphic presentations.

- TECHNICAL MEMORANDUM. Scientific and technical findings that are preliminary or of specialized interest, e.g., quick release reports, working papers, and bibliographies that contain minimal annotation. Does not contain extensive analysis.

- CONTRACTOR REPORT. Scientific and technical findings by NASA-sponsored contractors and grantees.

- CONFERENCE PUBLICATION. Collected papers from scientific and technical conferences, symposia, seminars, or other meetings sponsored or cosponsored by NASA.

- SPECIAL PUBLICATION. Scientific, technical, or historical information from NASA programs, projects, and missions, often concerned with subjects having substantial public interest.

- TECHNICAL TRANSLATION. English-language translations of foreign scientific and technical material pertinent to NASA's mission.

Specialized services also include creating custom thesauri, building customized databases, organizing and publishing research results.

For more information about the NASA STI program, see the following:

- Access the NASA STI program home page at *http://www.sti.nasa.gov*

- E-mail your question via the Internet to *help@sti.nasa.gov*

- Fax your question to the NASA STI Help Desk at 301–621–0134

- Telephone the NASA STI Help Desk at 301–621–0390

- Write to:
  NASA Center for AeroSpace Information (CASI)
  7115 Standard Drive
  Hanover, MD 21076–1320
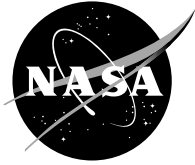
# Investigating Holey Metamaterial Effects in Terahertz Traveling-Wave Tube Amplifier

*David P. Starinshak*
*Ohio Aerospace Institute, Brook Park, Ohio*

*Jeffrey D. Wilson*
*Glenn Research Center, Cleveland, Ohio*

*Christine T. Chevalier*
*Analex Corporation, Cleveland, Ohio*

## Acknowledgments

The authors thank Dr. Carol L. Kory and Nathan D. Smith for valuable discussions.

# Investigating Holey Metamaterial Effects in Terahertz Traveling-Wave Tube Amplifier

David P. Starinshak
Ohio Aerospace Institute
Brook Park, Ohio 44142

Jeffrey D. Wilson
National Aeronautics and Space Administration
Glenn Research Center
Cleveland, Ohio 44135

Christine T. Chevalier
Analex Corporation
Cleveland, Ohio 44135

## Summary

Applying subwavelength holes to a novel traveling-wave tube amplifier is investigated. Plans to increase the on-axis impedance are discussed as well as optimization schemes to achieve this goal. Results suggest that an array of holes alone cannot significantly change the on-axis electric field in the vicinity of the electron beam. However, models of a beam tunnel with corrugated walls show promise in maximizing the amplifier's on-axis impedance. Additional work is required on the subject, and suggestions are made to determine research directions.

## Introduction

Considerable attention has been directed recently to the study of periodic arrays of subwavelength holes and their effects on transmitting and propagating specific wavelengths of electromagnetic radiation. For instance, the resonant behavior of surface currents for periodic geometries has been understood for many years and is central to the study of frequency selective surfaces (ref. 1). Moreover, recent investigations into the excitation of surface plasmons for a perforated thin metal sheet have demonstrated complete transmission of light for specific wavelengths—so called "Extraordinary Optical Transmission" (ref. 2). Further, layered arrays of subwavelength holes have been shown to exhibit negative-index propagation effects for certain electromagnetic frequencies (ref. 3). These findings reinforce Pendry's seminal work in surface plasmon excitation (ref. 4). Essentially, any conducting surface can be structured with vacuum or dielectric holes of specific dimensions to excite surface modes on the conductor (ref. 4). This report will investigate applying such subwavelength holes to improve the performance of a proposed 0.4-THz traveling-wave tube (TWT) amplifier.

The slow-wave circuit of the amplifier under investigation consists of a serpentine-shaped folded waveguide with a center-mounted, square beam tunnel. A schematic is shown in figure 1, with blue and yellow representing vacuum and perfect electric conductor (PEC), respectively. A rectangular coordinate system has been selected such that the origin sits at the center of the beam tunnel. The z-axis, which points down the beam tunnel, will be referred to as the axial direction. Also, the x- and y-axes are oriented parallel to the circuit face and will often be referred to as the horizontal and vertical directions, respectively. Modeling was completed using CST Microwave Studio's eigenmode solver (ref. 5).

For a given current and circuit length, it has been verified that the power output of a TWT amplifier depends strongly on the on-axis impedance of the device (ref. 6). For the $n$th space harmonic, the impedance is given by

$$K_n = \frac{E_n^2}{2\beta_n{}^2 P_{RF}} \tag{1}$$

where $P_{RF}$ refers to the RF power flow through the circuit, $\beta_n$ is the $n$th axial phase constant, and $E_n$ is the magnitude of the on-axis electric field for the $n$th harmonic (ref. 6). Since a larger impedance leads to an increase in electron beam interaction, improvements on the device center around increasing the magnitude of the axial electric field inside the beam tunnel.

Our approach to increasing the axial electric field in the beam tunnel involves adding subwavelength holes to the walls of the waveguide. Each hole acts as a rectangular waveguide with electric fields perpendicular to the waveguide surface. This causes the electric field to be at an angle to the surface. This is demonstrated in figure 2: figure 2(a) shows that in a surface without holes the electric field is perpendicular to the surface while figure 2(b) shows that a hole causes the electric field to be at an angle to the surface in the vicinity of the hole. By modifying the boundary conditions in this manner, we investigate developing configurations of holes to increase the magnitude of the axial electric field inside the beam tunnel. In addition, the possibility of achieving resonance both inside a single hole and among many holes in an array will be investigated to further enhance this effect.

## Hole Geometry

The geometry of the folded waveguide limits the locations in which holes can be placed. In an ideal case, the beam tunnel would be surrounded by an axially symmetric array of holes; however, the curved geometry of the waveguide creates two major challenges. First, it is difficult to quantitatively judge changes to boundary conditions along a curved surface. And second, microfabricating such a complicated geometry would be difficult. Hence, this study is limited to areas where the waveguide surface is flat. In particular, two rectangular regions with width $W$ and length $L$ exist to the left and right of the beam tunnel (see fig. 3). Holes added to these areas run parallel to the axis of the beam tunnel and pass through the entire length of the circuit.

To model the holes, a simple lattice array was selected as a template (see fig. 4). This geometry makes good use of the available space, is easily parameterized for optimization, and is simple to fabricate. In addition, seven variables were declared to define the hole structure. Parameters $l$ and $w$ describe the horizontal (x-direction) and vertical (y-direction) size of each hole, respectively; $h_b$ and $v_b$ define the horizontal and vertical space between holes, respectively; $n$ is the number of holes in the horizontal direction (the number of columns); $m$ is the number in the vertical direction (the number of rows); and $s$ describes the horizontal distance between the hole array and the sides of its bounding region. No vertical space is needed between the array and the top and bottom of the bounding region. Finally, the variables must satisfy the following constraints:

$$2s + nl + (n-1)h_b = L \qquad (2)$$

$$mw + (m-1)v_b \leq W \qquad (3)$$

with all values nonnegative. The studies included in this paper involve only a single row of holes, so the values of $m$ and $v_b$ are 1 and 0, respectively. Also, it should be noted that although the results of only a single row of holes are discussed here, it is assumed that increasing the number of holes will produce even greater electric field shaping.

## Testing Hole Effectiveness

Three methods were utilized to measure the effects of holes. First, a qualitative approach was taken to analyze how the electric field was shaped. For various hole configurations, surface contour plots of the axial electric fields were taken. In addition, arrow plots of the electric field vectors were analyzed at the interface between the holes and the folded waveguide. Microwave Studio normalizes each field to a particular mesh and volume, so different hole configurations will result in different magnitudes and scales. Thus to compare the effect of holes, we compute the electric field contours of a structure with holes on one side and no holes on the other side.

The second approach gives a quantitative approximation of the holes' effectiveness. As stated above, the axial electric field at the hole-waveguide interface must be comparable in magnitude to the perpendicular (y-direction) field set up inside the hole. Therefore, two pieces of information are needed to make an assessment: (1) the strength of the perpendicular y-field at the hole-waveguide interface and (2) the strength of the axial field if there were no holes present.

Just as with the contour plots, holes are placed on only one side of the beam tunnel. Area integrals are then taken on the holed and nonholed sides of the circuit. First, the square of the y-component of the electric field is integrated over the cross section of each hole along the interface. This integral will be referred to as $E_y^2$. The same is then done for the square of the z-component on the nonholed side, integrated over the same area as $E_y^2$. Likewise, this integral is referred to as $E_z^2$. The quantitative expression of interest is the ratio of these two values $E_z^2 / E_y^2$. Note that the smaller the value for this expression, the more the boundary condition is changed.

The third approach involves calculating the on-axis interaction impedance. For this method holes are placed on both sides of the beam tunnel. In addition, periodic boundaries are used in Microwave Studio. The results are compared to the impedance of the circuit with no holes on the sides of the beam tunnel.

# Methodology and Results

Initial investigations involved qualitative effects of various hole configurations on the shape of the axial electric field inside the circuit.

In order to test the behavior of holes with relatively small dimensions, a 3 by 3 square array was modeled (see fig. 5). A simple parameterization was used for this test: $D$ and $S$ were the lattice constants of the array and the side length of a single hole, respectively. The constant $D$ was held fixed at 5 μm, while $S$ took four values smaller than $D$. For each of four parameter combinations, no appreciable change in the axial electric field was observed, indicating that small holes are unable to adequately change the waveguide's boundary conditions.

Further qualitative measurements of the circuit's internal electric field indicated that longer holes (more accurately referred to as slots) are more likely to change boundary conditions. Three runs were set up to demonstrate this point; their parameter values can be found in table I. With the geometry illustrated in figure 6, contour plots of the axial (z-) component (fig. 7) and vertical (y-) component (fig. 8) were generated for the electric field. In figure 7, we observe greater shaping of axial fields inside the waveguide for a single wide slot than several shorter holes. Likewise, in figure 8, we find that stronger y-directed fields exist at the waveguide interface for slots than for holes. Therefore, a single slot of length $1.4W$ demonstrates the greatest potential to shape electric field vectors along the waveguide walls. One reason for this

phenomenon is the fact that field components are in competition inside a hole. To explain, field vectors must point normal to the surfaces of a hole. Thus, longer slots in the x-direction have larger surface areas on the top and bottom of the hole. Since the y-directed field points normal to these surfaces, a larger surface area means a stronger y-component at the waveguide interface. Similarly, holes with a longer width in the y-direction create more surface area along the sides of the hole, thus maximizing the x-component of fields. Additionally, both the x- and y-fields must also compete with the strong axial fields just outside the hole. As $l$ decreases, perpendicular y-fields inside the hole should become dominated by stronger axial fields from inside the waveguide.

To verify these observations quantitatively, a single hole was modeled with $w = 0.10W$. Then $L$ was allowed to vary from $0.20W$ to $1.40W$, with $E_z^2/E_y^2$ calculated for each parameter value. Figure 9 indicates that as the length of a hole increases with a fixed width, the axial and perpendicular fields become more comparable in magnitude.

If indeed the electric field components are in competition at the hole-waveguide interface, then for a given hole length, there may be an optimal width such that $E_z^2/E_y^2$ is smallest. To test this hypothesis, three runs were set up. A single hole was modeled with $length = 0.25W$, $0.50W$, and $1.00W$ and $w$ varying from $0.05W$ to $0.30W$. A plot of $E_z^2/E_y^2$ versus width is shown in figure 10 for each length. As expected, $E_z^2/E_y^2$ reaches a minimum value, representing an optimal hole width per length. In particular, for lengths of $0.25W$, $0.50W$, and $1.00W$, the most effective widths are $0.09W$, $0.14W$, and $0.19W$, respectively. Three important trends can be taken from this data: first, longer holes support stronger perpendicular fields; second, longer holes have a larger optimal width; and third, the minima of the curves becomes less defined for longer hole lengths. The first trend verifies our qualitative results, while the second one tells us there is a tradeoff between the effectiveness of holes and the amount of available space. The third, however, has implications in the fabrication process. A less-defined optimum means that the accuracy of microfabrication will not become an issue; even if hole dimensions are slightly off, their effectiveness will not change significantly.

Although subwavelength slots are capable of reducing axial electric fields along the waveguide surface, an appreciable change in these fields along the center of the circuit's beam tunnel has yet to be found. As figure 11 illustrates, field lines can be drastically reshaped along the hole-waveguide interface with just a single slot on each side, but fields inside the beam tunnel remain virtually unaffected. This was confirmed by calculating the on-axis impedance for the cases shown in figure 9. In addition to the data for a hole width of $0.10W$, the on-axis impedance was also calculated for a hole width of $0.25W$. The impedance values were normalized to the impedance of the TWT with no holes. The normalized values are plotted in figure 12.

In addition, changes to the angular geometry of the beam tunnel do not affect the axial electric field inside. Simulations featuring either a circular beam tunnel or a square one with rounded edges at the waveguide intersection exhibited no appreciable change in the central on-axis field. Such results indicate that boundary conditions must also be changed along the beam tunnel walls to achieve the desired electric field shaping. Three ideas worth investigating involve enhancing two of the beam tunnel's walls with either a dielectric or metamaterial substrate, a thin "uniplanar photonic band-gap structure" (ref. 7), or a series of subwavelength corrugations (ref. 8).

To investigate the first two ideas, software that supports negative values of permittivity and permeability for both user-defined materials and thin film boundary conditions will be needed to model beam tunnel enhancements. COMSOL's finite-element software Multiphysics shows potential to successfully complete these models (ref. 9).

As for the corrugated beam tunnel, a few preliminary qualitative tests were run. It was determined that shallow corrugations alone do not significantly affect fields along the beam tunnel. Consequently, it is estimated that corrugation depth should be at least about one quarter of the operating wavelength to make a noticeable difference. However, since deep corrugations are weak structurally, we instead investigated shallow corrugations in conjunction with slots (see fig. 13). We claim that the presence of slots will create boundary conditions similar to the corrugations, thus causing the electric field to react as though there was one long, continuous corrugation. On a qualitative level, this claim was verified: the relative field strength inside the beam tunnel did increase, more so than any uncorrugated geometry modeled (see fig. 14). Quantitative evidence of a change in the circuit's impedance is still pending, though. Overall, more work is needed to determine the effectiveness of a corrugated beam tunnel. Parameterization and optimization plans are underway, and a proposed model for future simulations is presented (fig. 15). It is assumed that by integrating a shallow corrugation with a holey waveguide, field shaping can be localized to the beam tunnel to effectively change impedance.

## Conclusions

The addition of subwavelength holes into a 0.4-THz traveling-wave tube amplifier has been investigated. The holes have demonstrated the ability to weakly change boundary conditions along the flat surfaces of a folded waveguide. As a result, controlled shaping of the electric field has been observed, with axial fields reduced at the hole-waveguide interface. Unfortunately, for every simulation, no significant change in the axial field's magnitude was observed inside the beam tunnel. Therefore, no significant change to the on-axis impedance has been achieved with the addition of subwavelength holes.

Future work on this subject will involve optimizing array dimensions, making changes to facilitate microfabrication, and modifying the beam tunnel to reshape axial fields. It has been found that a single long slot can support stronger perpendicular fields and better reduce axial fields than a series of shorter holes can. The tradeoff for better performance is structural weakness—a column of slots takes away too much of the circuit's structural support, making fabrication a problem. For that reason, work is being done to test if the effects of a slot can be duplicated by a single row of holes with the same combined length. If not, a middle ground must be reached to balance performance and support.

Investigating alternative hole shapes may also prove fruitful. So far, attention has only been paid to rectangular holes oriented horizontally. Vertical holes—rectangles with width greater than length—have not been seriously considered despite them having a distinct structural advantage over horizontal holes. Unlike previous tests, the effectiveness of vertical holes depends on the strength of the x-directed electric field inside. Furthermore, both qualitative and quantitative results are lacking with regards to how changing boundary conditions in the x-direction of the waveguide changes the axial field. Therefore, we would like to determine the effect hole placement has on the ratio of the axial electric field to the x-directed field as well as determine its usefulness as a quantitative measure.

Finally, preliminary computations suggest that corrugations on the beam tunnel walls warrant further investigation.

# References

1. Vardaxoglou, John C.: Frequency Selective Surfaces: Analysis and Design. Research Studies Press, New York, NY, 1997.
2. Beruete, M., et al.: Enhanced Millimeter Wave Transmission Through Quasioptical Subwavelength Perforated Plates. IEEE Trans. Antennas Propagation, vol. 53, no. 6, 2005, pp. 1897–1903.
3. Beruete, M.; Sorolla, M.; and Campillo, I.: Inhibiting Left-Handed Wave Propagation by a Band Gap of Stacked Cut-Off Metallic Hole Arrays. IEEE Microwave Wireless Comp. Letters, vol. 17, no. 1, 2007, pp. 16–18.
4. Pendry, J.B.; Martin-Moreno, L.; and Garcia-Vidal. F.J.: Mimicking Surface Plasmons With Structured Surfaces. SCI., vol. 305, no. 5685, 2004, pp. 847–848.
5. CST Design Studio. Computer Simulation Technology, Sept. 2005.
6. Pierce, John Robinson: Traveling-Wave Tubes. Van Nostrand, New York, NY, 1950.
7. Yang, F.R., et al.: A Novel TEM Waveguide Using Uniplanar Compact Photonic Bandgap (UC–PBG) Structure. IEEE Trans. Microwave Theory Tech., vol. 47, no. 11, 1999, pp. 2092–2098.
8. Dybdal, R.B.; Peters, L., Jr.; and Peake, W.H.: Rectangular Waveguides With Impedance Walls. IEEE Trans. Microwave Theory Tech., vol. MTT−19, no. 1, 1971, pp. 2–9.
9. COMSOL Multiphysics User's Guide. Version 3.2, COMSOL AB, Sept. 2005.

TABLE I.—PARAMETER VALUES FOR THREE SINGLE-ROW HOLE ARRAYS IN TRAVELING-WAVE TUBE CIRCUIT[a]

[Vertical space between holes $v_b = 0$.]

| Runs | Number of hole columns, $n$ | Number of hole rows, $m$ | Length of hole,[b] $l$ | Width of hole,[b] $w$ | Horizontal space between holes,[b] $h_b$ | Spacer,[b] $s$ |
|---|---|---|---|---|---|---|
| Single slot | 1 | 1 | 1.40$W$ | 0.10$W$ | ---- | 0.10$W$ |
| Two-hole setup | 2 | 1 | 0.675$W$ | 0.10$W$ | 0.05$W$ | 0.10$W$ |
| Four-hole setup | 4 | 1 | 0.275$W$ | 0.10$W$ | 0.10$W$ | 0.10$W$ |

[a]Parameters are shown in figure 4.
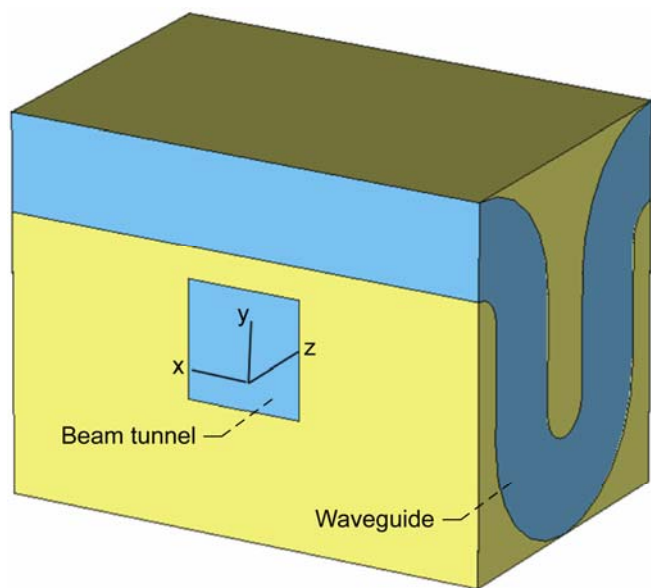[b]$W$ is width of rectangular section on either side of beam tunnel.

Figure 1.—Geometry for one period of 0.4-THz folded-waveguide traveling-wave tube. Vacuum structures are indicated by blue, whereas yellow areas are perfect electric conductors.
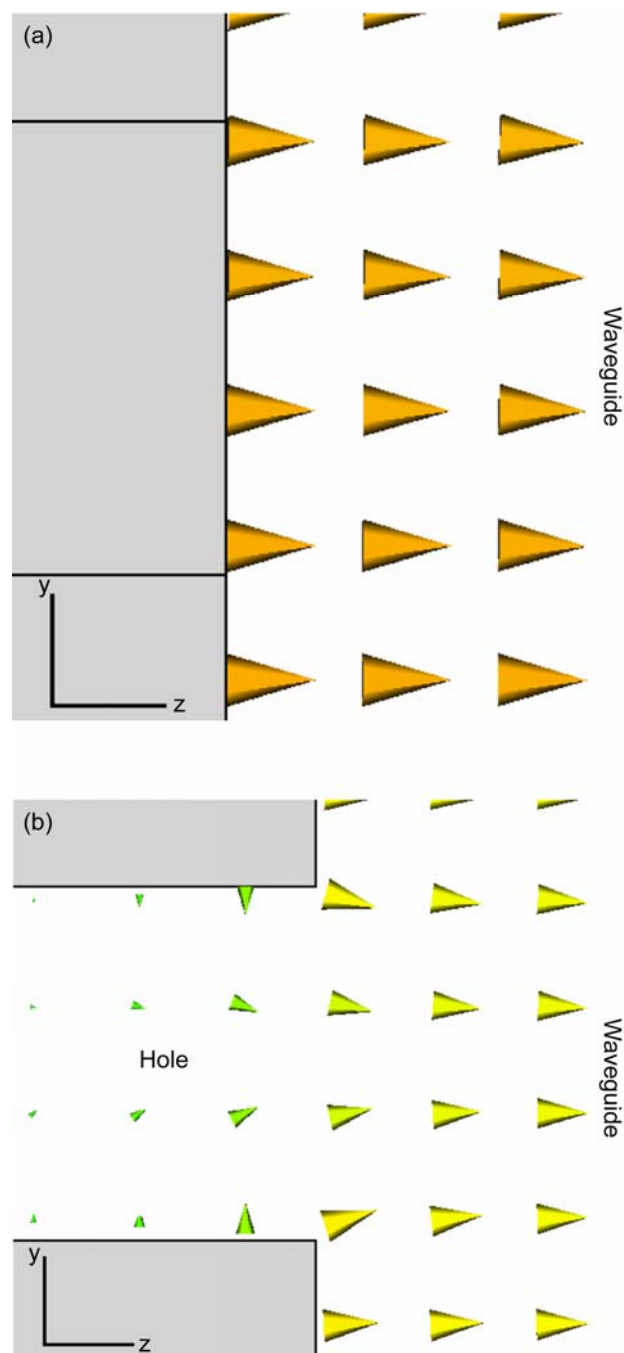


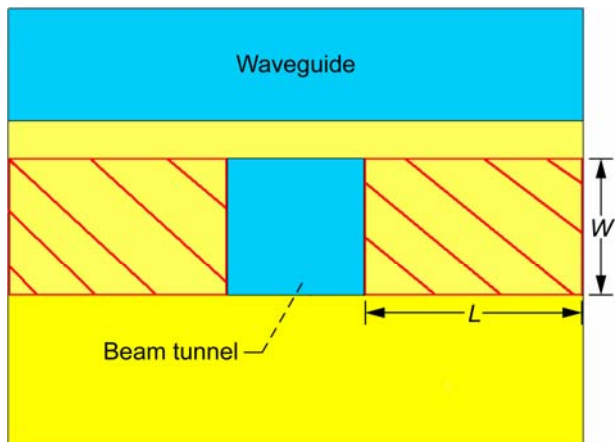Figure 2.—Comparison of electric field vectors along waveguide wall. (a) Without holes. (b) With holes.

Figure 3.—Front view of traveling-wave tube. Modeling of holes is limited to regions in red.
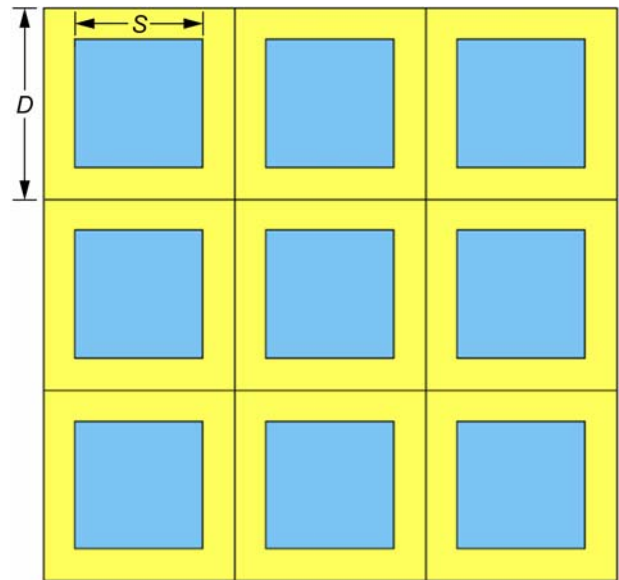


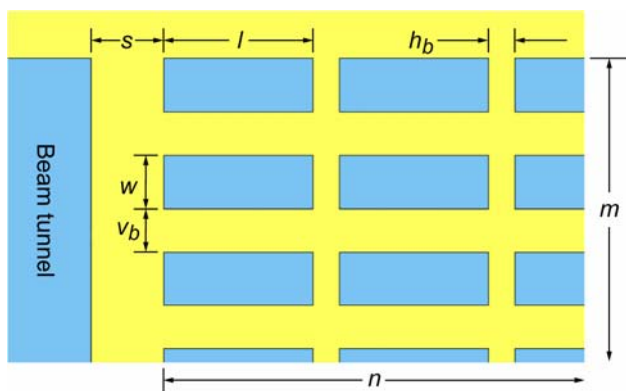Figure 5.—Traveling-wave tube circuit 3 by 3 square hole array. $D$ was held constant, and $S$ took four values < $D$.



Figure 4.—Generalized rectangular hole array of traveling-wave tube amplifier with labeled parameters, where $n$ is the number of hole rows and $m$ is the number of hole columns.
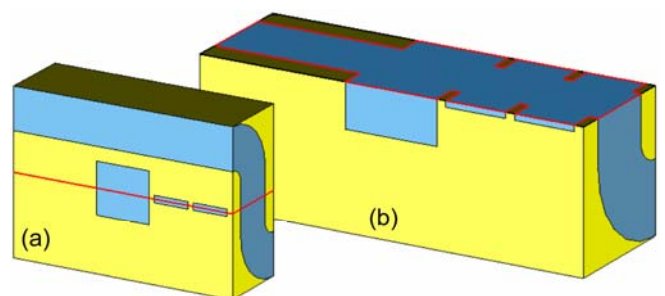


Figure 6.—One period of traveling-wave tube amplifier; geometry used for results in figures 7 and 8. (a) Cutting plane for two-dimensional contour plots. (b) View of circuit with top cut away.
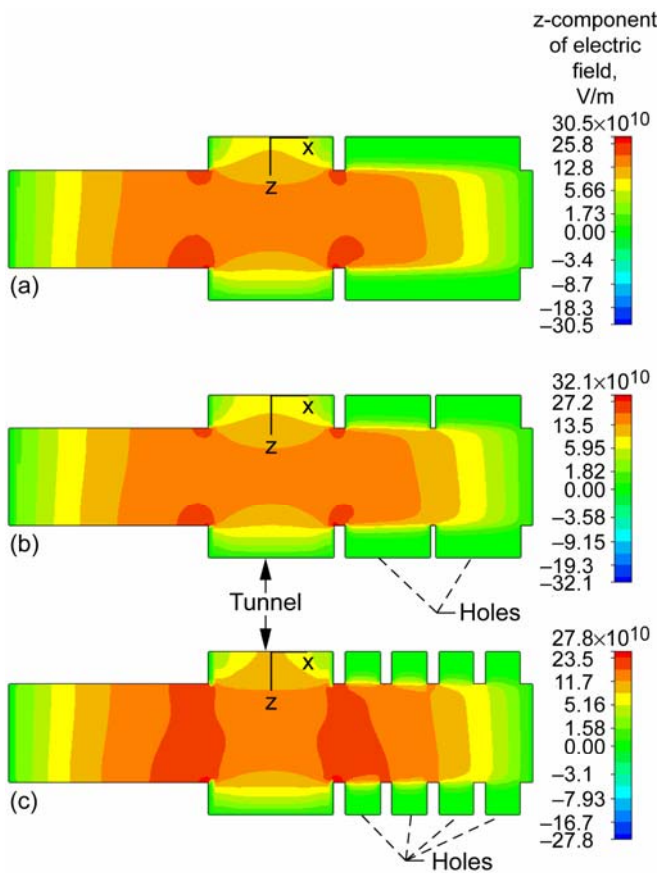
Figure 7.—Top view of z-component electric field inside one cavity of traveling-wave tube. Magnitude of z-component at hole-waveguide intersection. (a) Single long hole. (b) Two holes. (c) Four holes.
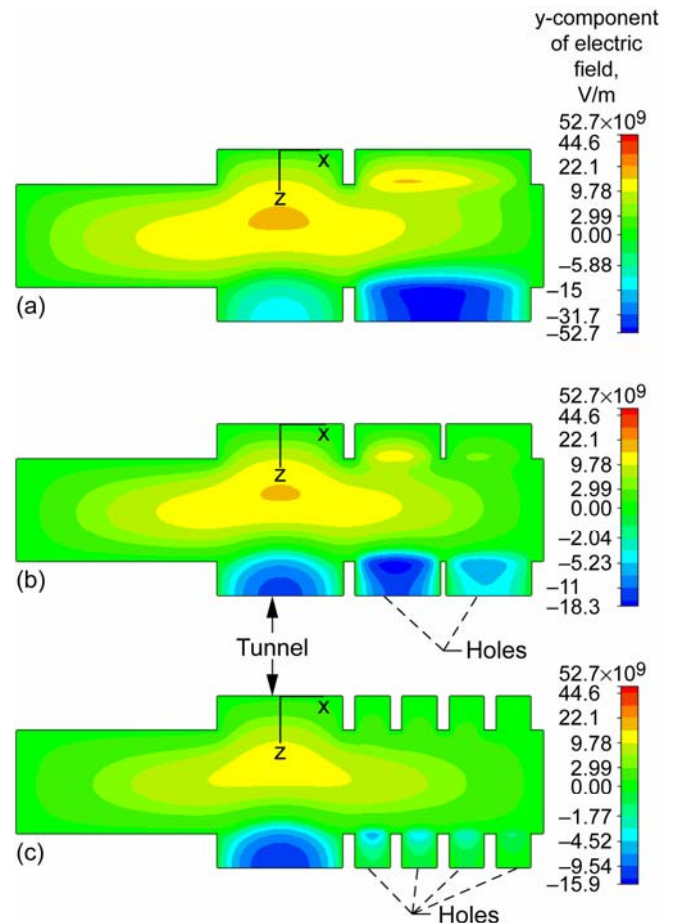


Figure 8.—Top view of y-component electric field inside one cavity of traveling-wave tube. Magnitude of y-component at hole-waveguide intersection. (a) Single long hole. (b) Two holes. (c) Four holes.
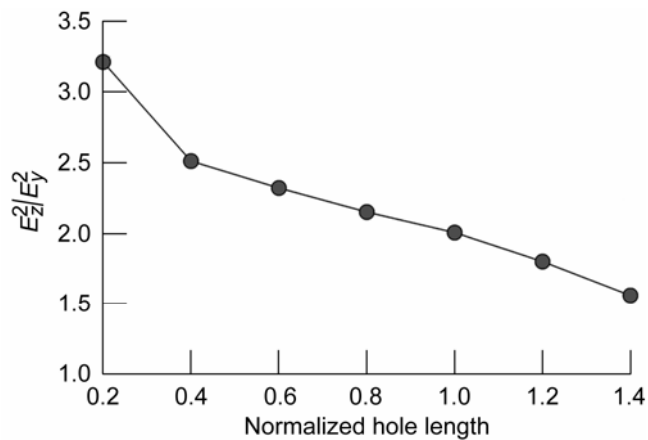
Figure 9.—Ratio of axial electric field to y-component of electric field $E_z^2/E_y^2$ calculated for single hole of width $0.10W$ and varying length. Normalization is with respect to width of rectangular sections on either side of beam tunnel $W$.
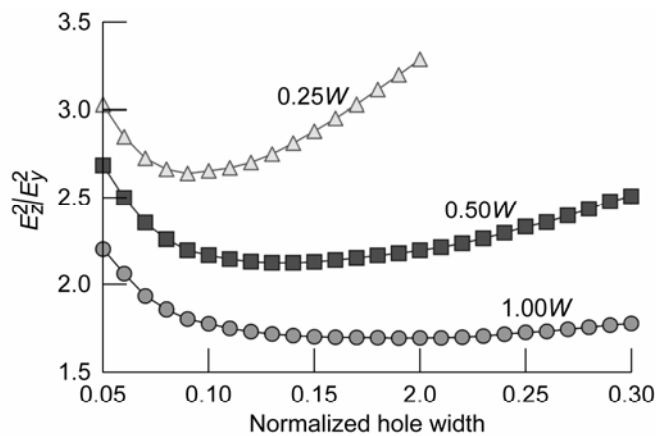


Figure 10.—Ratio of axial electric field to y-component of electric field $E_z^2/E_y^2$ versus normalized hole width for length of hole = $0.25W$, $0.50W$, and $1.00W$, where $W$ is width of rectangular sections on either side of beam tunnel. Minima represent the optimal width for a given length.
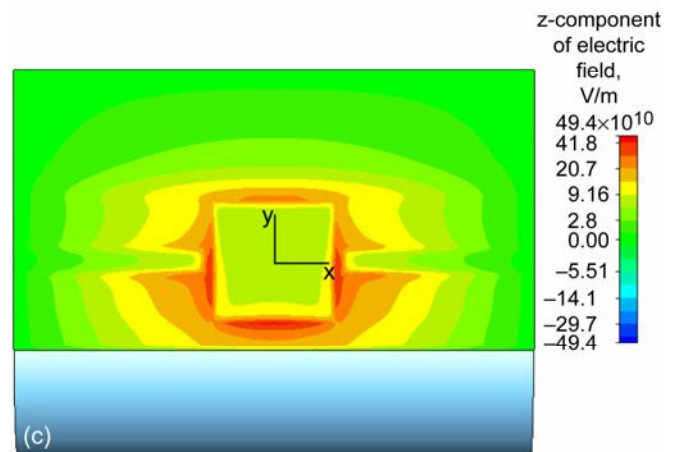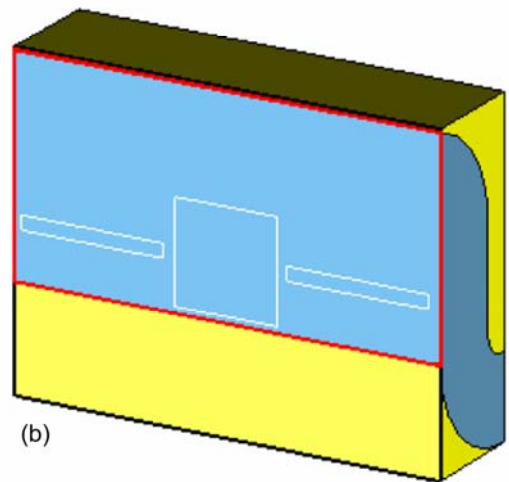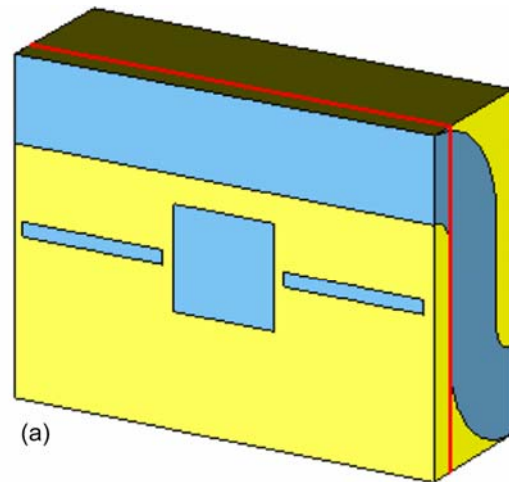


Figure 11.—Front view of axial field at hole-waveguide inter-section. A single hole is modeled on each side of beam tunnel. (a) Cutting plane for two-dimensional contour plots. (b) Traveling-wave tube with front cut away. (c) Axial electric field contours.
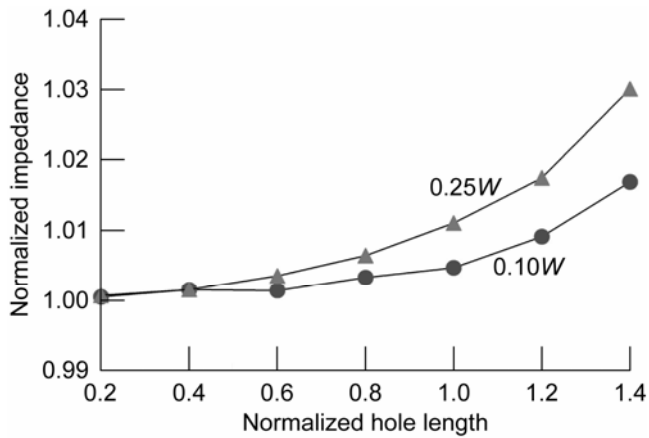
Figure 12.—Normalized on-axis interaction impedance versus normalized hole length for width $w = 0.10W$ and $0.25W$, where $W$ is width of rectangular sections on either side of beam tunnel.
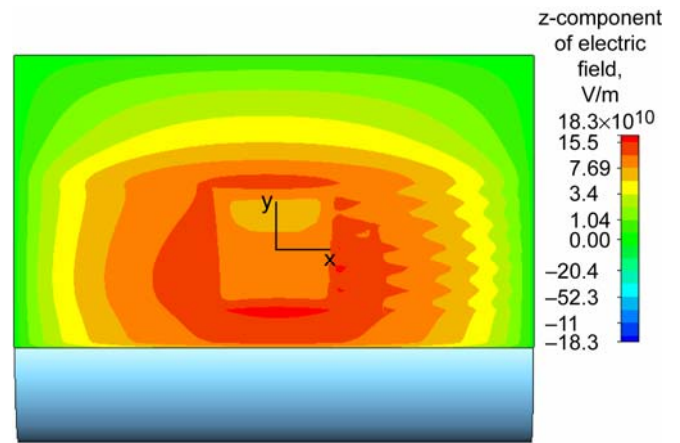


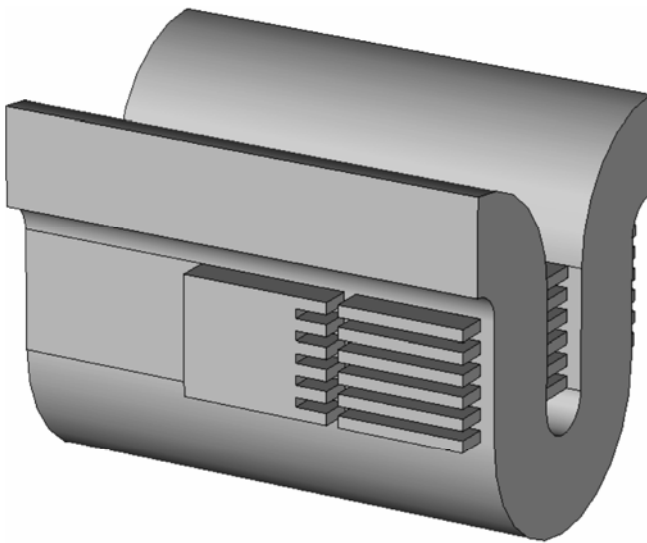Figure 14.—Front view of axial field at hole-waveguide inter-section for geometry in figure 13.



Figure 13.—Traveling-wave tube slow-wave circuit with corrugated beam tube and slots, both of equal width and spacing. The opposite half of circuit is left unchanged for purpose of comparison.
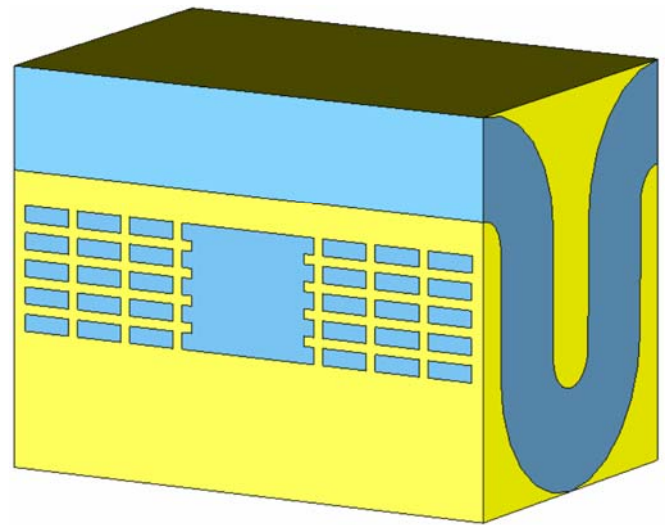


Figure 15.—Proposed holey folded-waveguide traveling-wave tube slow-wave circuit with corrugated beam tunnel.

| **1. REPORT DATE** *(DD-MM-YYYY)* <br> 01-09-2007 | **2. REPORT TYPE** <br> Technical Paper | **3. DATES COVERED** *(From - To)* |
|---|---|---|

| **4. TITLE AND SUBTITLE** <br> Investigating Holey Metamaterial Effects in Terahertz Traveling-Wave Tube Amplifier | **5a. CONTRACT NUMBER** |
|---|---|
| | **5b. GRANT NUMBER** |
| | **5c. PROGRAM ELEMENT NUMBER** |
| **6. AUTHOR(S)** <br> Starinshak, David, P.; Wilson, Jeffrey, D.; Chevalier, Christine, T. | **5d. PROJECT NUMBER** |
| | **5e. TASK NUMBER** |
| | **5f. WORK UNIT NUMBER** <br> WBS 953033.01.03.45 |

| **7. PERFORMING ORGANIZATION NAME(S) AND ADDRESS(ES)** <br> National Aeronautics and Space Administration <br> John H. Glenn Research Center at Lewis Field <br> Cleveland, Ohio 44135-3191 | **8. PERFORMING ORGANIZATION REPORT NUMBER** <br> E-15902 |
|---|---|

| **9. SPONSORING/MONITORING AGENCY NAME(S) AND ADDRESS(ES)** <br> National Aeronautics and Space Administration <br> Washington, DC 20546-0001 | **10. SPONSORING/MONITORS ACRONYM(S)** <br> NASA |
|---|---|
| | **11. SPONSORING/MONITORING REPORT NUMBER** <br> NASA/TP-2007-214701 |

**12. DISTRIBUTION/AVAILABILITY STATEMENT**
Unclassified-Unlimited
Subject Category: 32
Available electronically at http://gltrs.grc.nasa.gov
This publication is available from the NASA Center for AeroSpace Information, 301-621-0390

**13. SUPPLEMENTARY NOTES**

**14. ABSTRACT**
Applying subwavelength holes to a novel traveling-wave tube amplifier is investigated. Plans to increase the on-axis impedance are discussed as well as optimization schemes to achieve this goal. Results suggest that an array of holes alone cannot significantly change the on-axis electric field in the vicinity of the electron beam. However, models of a beam tunnel with corrugated walls show promise in maximizing the amplifier's on-axis impedance. Additional work is required on the subject, and suggestions are made to determine research directions.

**15. SUBJECT TERMS**
Traveling wave tubes; Circuits; Electromagnetic fields; Millimeter waves; Metamaterials; Terahertz waves

| **16. SECURITY CLASSIFICATION OF:** | | | **17. LIMITATION OF ABSTRACT** | **18. NUMBER OF PAGES** | **19a. NAME OF RESPONSIBLE PERSON** <br> STI Help Desk (email:help@sti.nasa.gov) |
|---|---|---|---|---|---|
| **a. REPORT** <br> U | **b. ABSTRACT** <br> U | **c. THIS PAGE** <br> U | UU | 15 | **19b. TELEPHONE NUMBER** *(include area code)* <br> 301-621-0390 |